Deformation Characteristics of Geomaterials
V.A. Rinaldi et al. (Eds.)
IOS Press, 2015
© 2015 The authors and IOS Press. All rights reserved.
doi:10.3233/978-1-61499-601-9-866

Advanced laboratory investigation of axial cyclic loading in silica sands

(*Dedicated to late Professor Pierre Foray*)

Cristina de H. C. TSUHA[a,1], Richard J. JARDINE[b], Zhongxuan YANG[c], Matias SILVA[d] and Siya RIMOY[e]

[a]*University of São Paulo, Department of Geotechnical Engineering, Brazil*
[b]*Imperial College, Department of Civil and Environmental Engineering, London*
[c]*Department of Civil Engineering, Zhejiang University, China*
[d]*Institut National Polytechnique de Grenoble, Laboratoire 3S-R, France*
[e]*University of Dar es Salaam, Department of Transportation and Geotechnical Engineering, Tanzania*

Abstract. This paper describes the global behaviour of and local stress conditions applying to highly instrumented cyclic laboratory model displacement pile tests conducted in a calibration chamber on medium dense Fontainebleau NE34 sand. The instrumentation provided measurements of the contact stresses on the jacked pile shaft and the local vertical, radial and circumferential stresses in the surrounding soil mass, in tests involving a range of cyclic load amplitudes. The patterns of effective stress developing on and around the pile shaft are described. The data obtained are interpreted by reference to cyclic soil element tests conducted on the same soil, as described in the parallel investigation by Aghakouchak et al (2015), reported in the same symposium. The calibration chamber experiments offer a comprehensive understanding of the cyclic degradation processes, and provide key information for improving the design of piled foundations under cyclic loading.

Keywords. Cyclic loading, pile–soil interface, calibration chamber, sand, local stresses

1. Introduction

The piled foundations of offshore platforms, wind turbines, and other types of structures are usually subject to significant environmental and operating axial load cycles. Such loading cycles can lead to changes in stiffness, permanent displacement growth and changes in axial capacity. Shaft resistance can either degrade markedly, or potentially improve [1], [2]. Field tests on piles driven in sands have identified three main styles of response to cyclic axial loading, which are dependent of the mean load,

[1] Corresponding Author: Cristina de Hollanda Cavalcanti Tsuha, University of São Paulo, Department of Geotechnical Engineering, Av. Trabalhador Sãocarlense, 400, São Carlos, SP 13566-590, Brazil; E-mail: chctsuha@sc.usp.br.

cyclic amplitude, and number of applied cycles. The responses thought to be linked to changes in the shaft radial effective stress distributions [3],[4]. Although potentially important, such effects are rarely addressed in routine offshore or onshore pile design.

The experimental program presented in this paper was developed to better characterize the three different cyclic behaviour styles and provide mechanical explanations for the processes involved, by measuring how stresses evolve at the displacement pile surface and in the surrounding sand mass under axial shaft loading.

The current study is a part of a joint research programme between the Laboratoire 3S-R (Grenoble Institute of Technology) and Imperial College London about displacement pile behaviour in medium dense sand. A highly instrumented steel pile Mini-ICP was developed by Imperial College of London and the experiments were conducted in a calibration chamber at the Grenoble Institute of Technology (INPG).

The key findings described in this text are based on the results obtained from four test series' Mini-ICP1, Mini-ICP2, Mini-ICP3 and Mini-ICP4. The Mini-ICP pile was installed into reconstituted siliceous Fontainebleau NE34 sand in the chamber tank. The vertical, radial and circumferential stresses (σ'_z, σ'_r, and σ'_θ) developed in the sand mass were measured by suites of sensors placed at up to three different levels.

2. Testing programme

2.1. Grenoble calibration chamber

The Grenoble calibration chamber (Figure 1) is 1.5 m high and 1.2 m in internal diameter. The chamber base and top cover consist of rigid plates with a 100 mm thickness. An upper membrane, filled with water, applies the vertical stress conditions (σ'_{vo} around 150 kPa for the present study), and a single latex rubber sheet smeared with silicone grease was employed to provide near K_0 conditions while reducing wall friction between the sand and the tank. The chamber tank was filled with NE34 Fontainebleau sand by air pluviation technique to provide a relative density of 72%. Table 1 shows the index properties of this sand. Independent standard CPT tests were conducted on sand samples under the same 150 kPa σ'_{vo}, and the cone end resistance (q_c) traces presented quasi-constant 21 ± 2 MPa sections. The mechanical properties of the sand are described in detail elsewhere [5].

Table 1. Fontainebleau NE34 sand

Grain shape	D_{10} (mm)	D_{50} (mm)	D_{60} (mm)	e_{max}	e_{min}
Sub-angular	0.15	0.21	0.23	0.90	0.51

2.2. Mini-ICP pile and soil sensors

The 36 mm-diameter closed-ended stainless steel Mini-ICP pile (Figure2) is composed of three instrumented clusters (leading or A, following or B, and trailing or C), a solid 60° cone fitted at the pile tip, and a pile cap. Each cluster contains an axial load cell (ALC), which can be used together with adjacent ALCs to derive the average pile skin friction; a surface stress transducer (SST) to measure radial, total stress (σ'_r) and shear stress (τ_{rz}); a temperature sensor; and inclinometers sensors. Further details of the Mini-ICP pile are given in [6].

The pressure sensors to monitor the stresses in the sand mass consist of disk-shaped cells (diameters of 6 to 6.5mm, and thicknesses of 0.6 to 1.4mm). The sensors faces were oriented in the direction of the normal stresses (σ'_z, σ'_r, and σ'_θ: vertical, radial and circumferential stresses, respectively). The special calibration procedures that are essential to interpret the soil sensors' complex behaviour are detailed in [7]. Figure 1 illustrates the sensor configuration for the Mini-ICP3 test. The relative radial distance of the sensors from the pile axis r/R varies from 2 to 20, as described in [6], where R is the pile radius and r is each sensor's radial distance from pile axis.

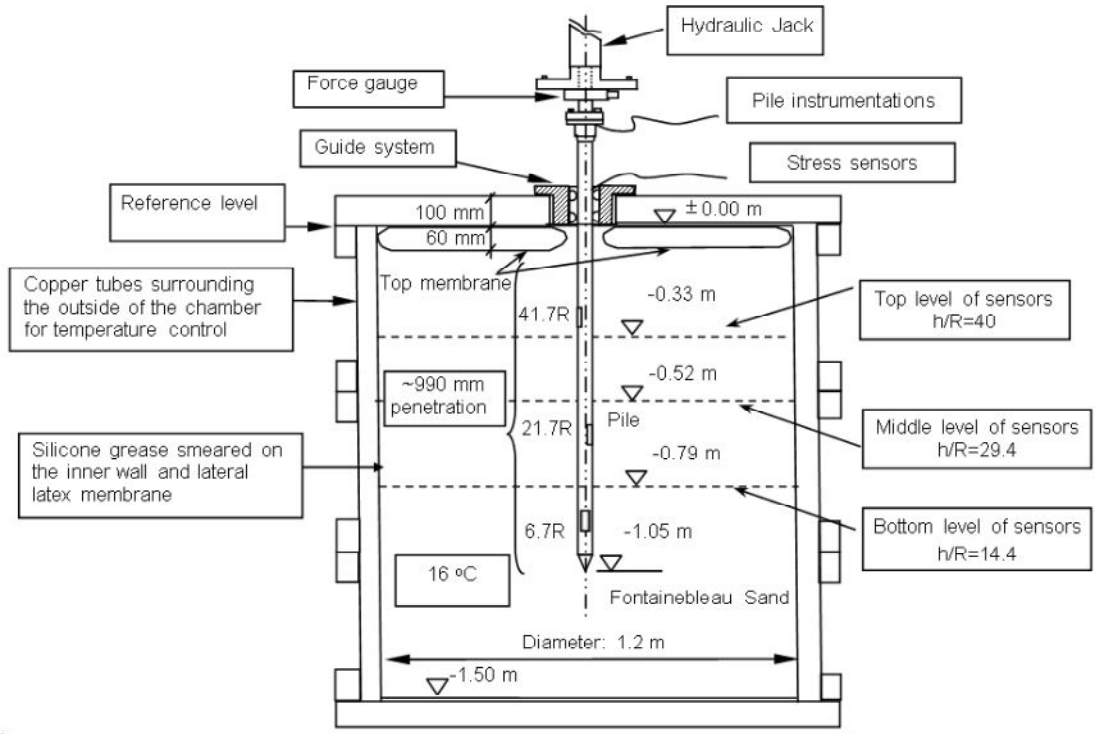


Figure 1. Typical arrangement for Mini-ICP tests.

2.3. Pile installation and cyclic loading tests

The Mini-ICPs were installed into the chamber tank by cyclic jacking to simulate key aspects of the driving process, by applying stroke lengths between 5 and 20 mm and reducing the pile head loads to zero at the end of each stroke. The final tip depths below sand surface were 0.92 m for Mini-ICP1, and 0.99 m for the other installations.

Static monotonic loading tests were carried out before and after each cyclic test to verify the cyclic loading influence on pile shaft capacity. The monotonic loading tests were performed under displacement control at rates around 0.01 mm/s. After these initial tests, series of tensile one-way cyclic loading were performed on Mini-ICP pile, under load-controlled conditions. Following the sequence of one-way cyclic tests, high-level two-way cyclic loading (both compression and tension) were conducted under either displacement or load-controlled conditions. Table 2 summarizes the cyclic testing programme and the results of pile tension capacity (Q_T) measured prior to the cyclic tests. The loading parameters in this table are normalised by Q_T.

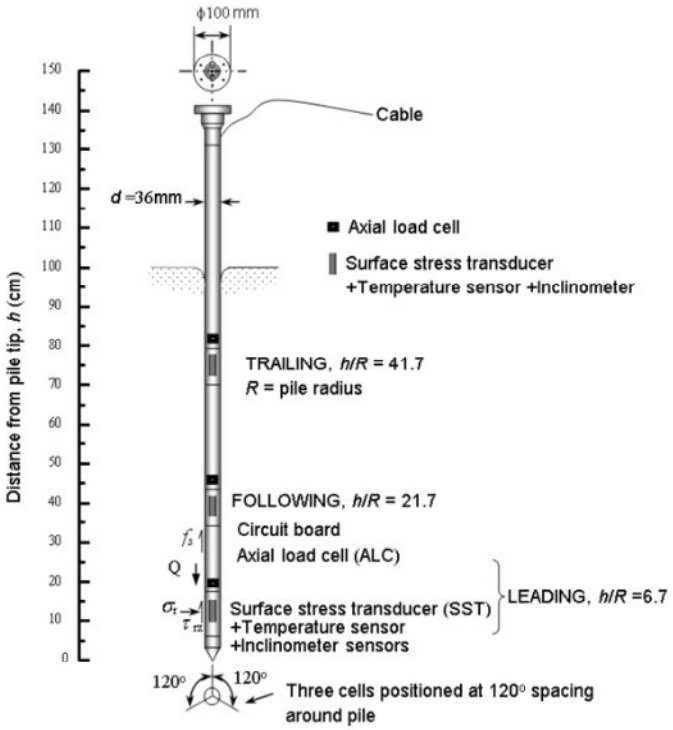


Figure 2. Mini-ICP1 configuration [6].

3. Pile cyclic axial response

In the current study, the classification of cyclic response is based on the number of cycles (N) necessary to cause either failure at the shaft-soil interface or specified rates of permanent displacement growth. In this case, cyclic failure occurs when accumulated displacement (s) reached 10% of the pile diameter or the rate ds/dN shows a sharp increase. Rates are considered slow if < 1 mm/10^4 cycles, and fast if > 1 mm/100 cycles). The 3 styles of response, identified in Figure 3, are then defined as:

- *Stable* if no failure occurs before 1000 cycles, with slow rates of permanent displacements.
- *Meta-Stable* if failure occurs with $100 < N < 1000$, with rates of permanent displacements fail to stabilise slow values.
- *Unstable* if failure develops before N =100.

Figure 3 presents a cyclic shaft failure interaction chart in which the cyclic loads are plotted as Q_{cyclic} and Q_{mean} normalised by the static failure load Q_T. The annotated numbers signify N_f - the number of uniform cycles required to induce a cyclic failure. Where no number is given, failure did not occur within at least 1000 cycles. Further details of the experiments are listed in Table 2. The pattern observed in Figure 3 is closely comparable to that reported from full-scale piles driven in sand [1], [2].

Three key aspects of each style of cyclic behaviour are illustrated in Figures 4, 5, and 6, covering *Stable*, *Meta-stable* and *Unstable* test outcomes respectively. The cumulative displacements under *Stable* (ICP4-OW1), *Meta-stable* (ICP2-OW3) and *Unstable* (ICP3-OW1) one-way cyclic experiments are shown in Figures 4a, 5a, and 6a. The corresponding pile surface effective stress paths, deduced from the surface stress

transducers, are given in Figures 4b, 5b, and 6b, which also indicate the estimated extent and position of the sand's initial Y_2 kinematic yield surfaces, as defined in [9].

Table 2. Mini-ICP cyclic loading details.

Installation	Test	No of cycles	Mean cyclic period *T* (min)	Q_T (kN)	Q_{cyclic}/Q_T	Q_{mean}/Q_T
Mini-ICP1	ICP1-OW1(Meta-stable)	1000	0.58	9.2	0.22	0.22
	ICP1-TW1 (Unstable)	100 (N_f=4)	2.64	10.8	0.41	0.06
Mini-ICP2	ICP2-OW1 (Stable)	1000	0.43	12.1	0.12	0.12
	ICP2-OW2 (Stable)	1000	0.70	13.2	0.20	0.20
	ICP2-OW3(Meta-stable)	500	1.04	14.0	0.28	0.28
	ICP2-TW1 (Unstable)	100 (N_f= 4)	2.17	13.7	0.48	0.15
Mini-ICP3	ICP3-OW1 (Unstable)	100(N_f=66)	1.64	12.5	0.38	0.38
	CP3-TW1 (Unstable)	1 (N_f= 1)	6	10.9	0.54	-0.08
	ICP3-TW2 (Unstable)	199(N_f=165)	0.73	10.9	0.40	0.06
	ICP3-TW2 (Unstable)	50 (N_f=10)	1.04	10.9	0.44	0.02
	ICP3-TW4 (Unstable)	37 (N_f= 3)	2.16	10.9	0.44	0.02
Mini-ICP4	ICP4-OW1 (Stable)	7000	0.43	11.5	0.15	0.15
	ICP4-TW1(Meta-stable)	600(N_f=580)	0.44	13.9	0.23	0.06
	ICP4-OW2 (Metastable)	50(incomplete)	0.18	5.5	0.21	0.63

*OW = one-way tension test; TW = two way compression/tension test.
** The control mode of these cyclic tests is described in [6].

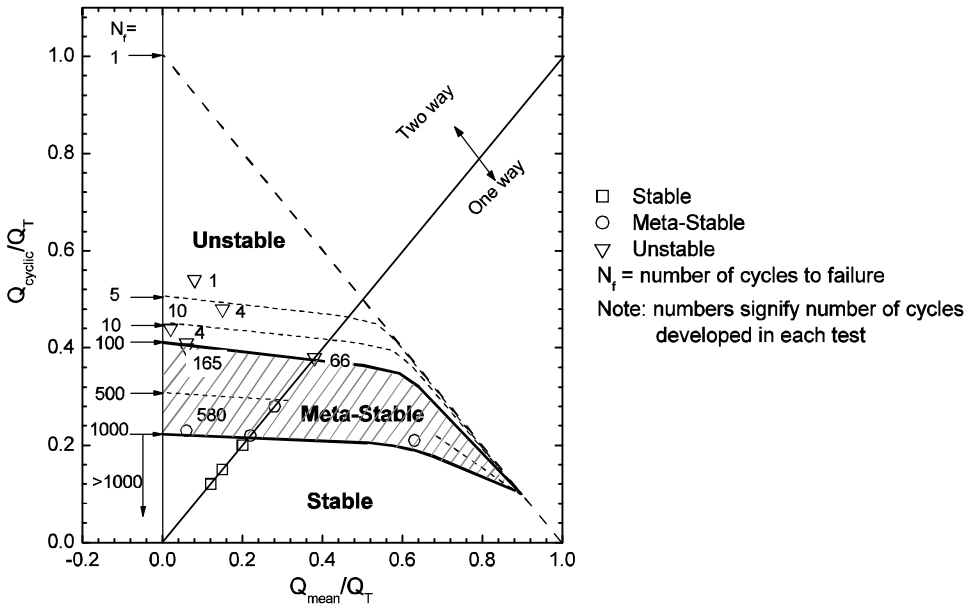


Figure 3. Summary of average cyclic shaft loading and failure conditions in Mini-ICP tests, showing Stable, Meta-Stable and Unstable Zone boundaries [6].

The Stable test presented in Figure 4b illustrates only slight top-down degradation with radial stresses reducing slowly as cycling continues. The local effective stresses remain principally within the sand's initial Y_2 yield surface. In contrast, the *Meta-stable* effective stress paths plotted in Fig 5b approach the static interface shear failure envelope, described by [5]. The *Unstable* response shown in Fig. 6b indicates effective stress paths that moved sharply to the left, engaging and relocating their Y_2 surfaces within the first cycle. Figures 4c, 5c, and 6c report the effective stress paths measured

at r/R=5 and h/R~15 in the sand mass by the sensors described in [8] under the same three styles of cyclic loading. In these figures, the initial Y_2 surface is represented by a circle with a radius of $0.245p'$, corresponding to the triaxial test range reported in [10].

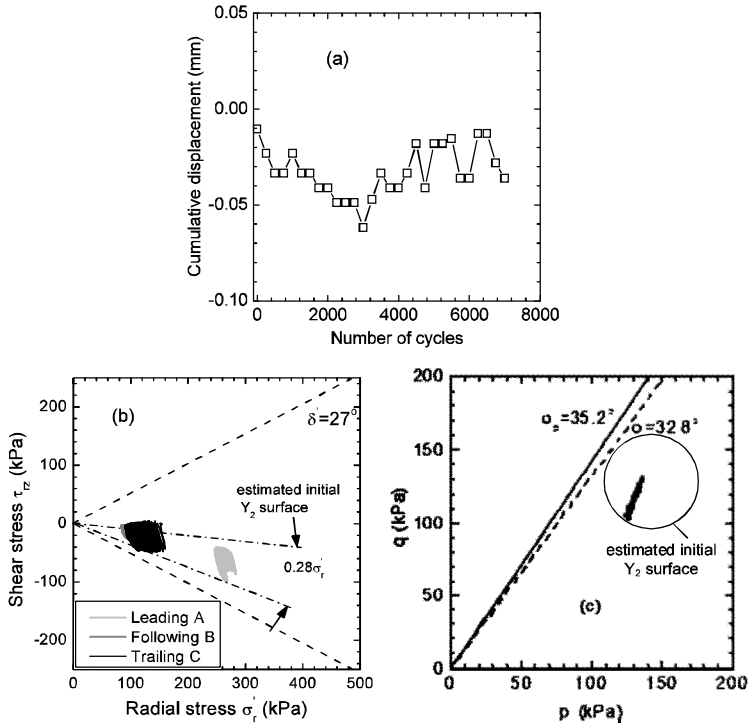


Figure 4. *Stable* test ICP4-OW1: (a) cumulative displacements, (b) effective stress paths at all SST's and (c) effective stress path developed in sand mass at 5*R*, *h*/*R*~15.

4. Effect of cyclic loading on shaft capacity

Tension pile tests demonstrated that capacity (Q_T) grew by up to 20% after prolonged *Stable* cycling (see Table 2). This is interpreted as being due to the densification in the interface zone and fabric rearrangement that increases dilation under static loading.

In contrast, two-way *Unstable* tests led to shaft capacities degrading by up to 50%. In the case of *Meta-stable* cycles, the shaft capacity reduction depended on the cyclic loading levels imposed. These features may be gauged by comparing the initial Q_T listed in Table 2 for tests ICP1-TW1, ICP2-TW1, ICP3-TW4 and ICP4-OW2 with their post cycling Q_T values of 4.9, 8.7, 4.8, and 6.0 kN respectively.

The laboratory piles' cyclic responses have been investigated by locally instrumented cyclic triaxial tests designed to model conditions around the pile shaft [11]. These special cyclic triaxial tests were carried out on specimens of NE34 Fontainebleau, prepared at similar relative densities (70%) to the calibration chamber tests. The samples were conditioned through controlled stages of consolidation to elevated pressures, prior drained triaxial cycling and extended ageing to simulate the pile installation process. Undrained cycling was then applied under a range of Cyclic Stress Ratios (CSR = q_{cyc}/p_0'). As with the pile tests, *Stable*, *Meta-stable* and *Unstable* responses were observed in terms of mean effective stress drift, cyclic stiffness and permanent strain growth. Such experiments provide a way of predicting field behaviour at sites where cyclic pile loading experiments are possible.

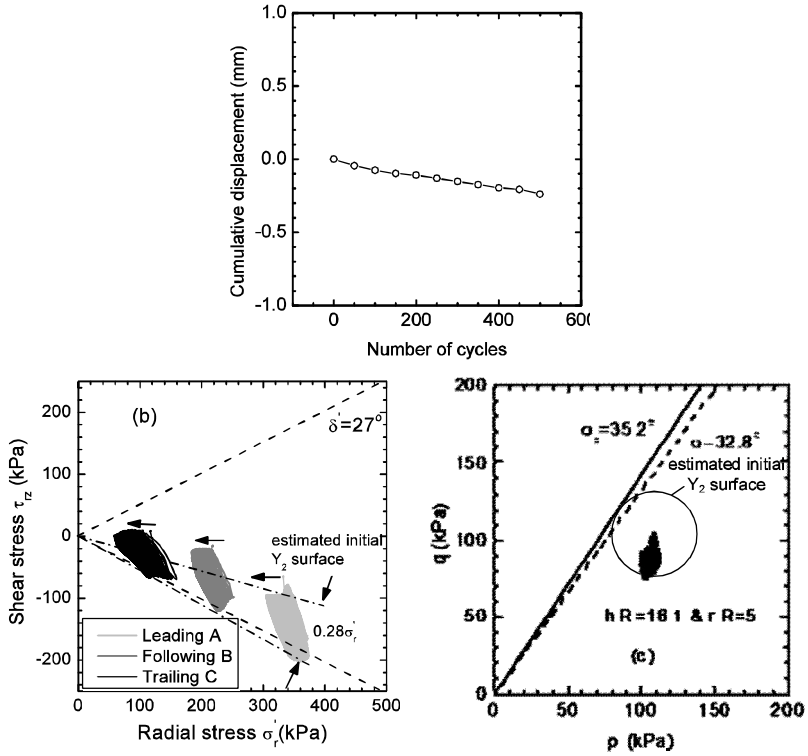


Figure 5. *Meta-Stable* test ICP2-OW3: (a) cumulative displacements, (b) effective stress paths at all SST's and (c) effective stress path developed in sand mass at 5*R*, *h*/*R*~15.

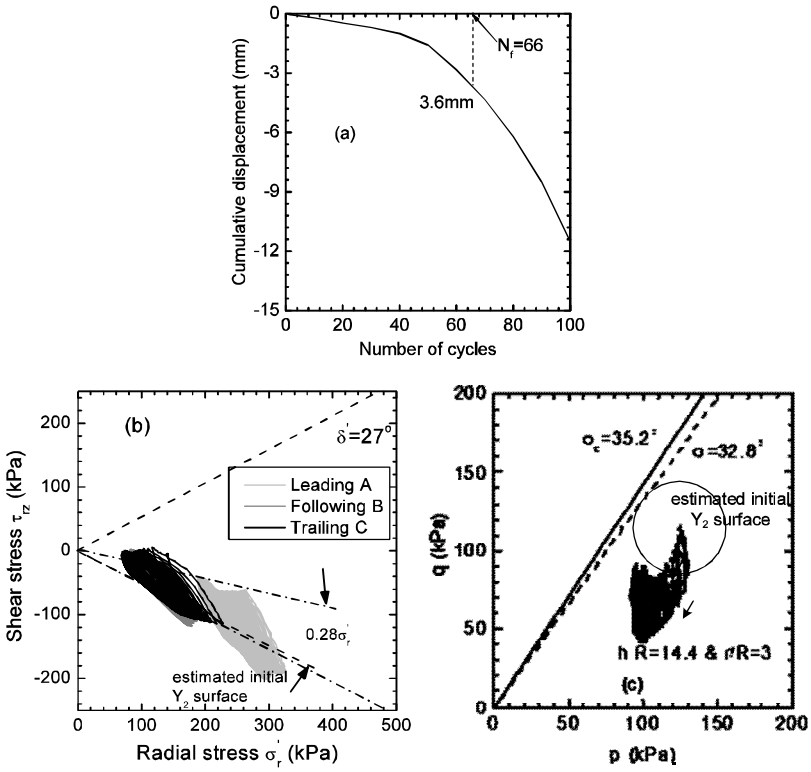


Figure 6. *Unstable* test ICP3-OW1: (a) cumulative displacements, (b) effective stress paths at all SST's and (c) effective stress path developed in sand mass at 5*R*, *h*/*R*~15.

5. Conclusions

Calibration chamber experiments on a model displacement pile jacked into a medium dense sand mass subjected to cyclic axial loading identify:

- The combinations of mean load, cyclic load, and number of cycles that lead to three distinct styles of pile response: Stable, giving no loss of shaft friction and possibly gains, Unstable, where shaft capacity falls sharply, and Meta-stable, where the shaft can sustain hundreds of such cycles before failing.
- Explanations for the responses seen in full scale field tests.
- Cyclic behaviours patterns that can be reproduced in appropriately designed special cyclic triaxial tests.
- Ways forward for practical cyclic design, as outlined in [12].

6. Acknowledgements

The authors gratefully acknowledge the support provided by Shell U.K. Limited, the UK Health and Safety Executive, the UK Engineering Physical Sciences Research Council, Total France, Centre National de la Recherche Scientifique (CNRS), and the French Program ANR SOLCYP.

References

[1] R.J. Jardine, & R.J. Standing. Pile Load Testing Performed for HSE Cyclic Loading Study at Dunkirk, France. Two Volumes. Offshore Technology Report OTO2000 007. Health and Safety Executive, London. 2000.

[2] R.J. Jardine R.J. and J.R. Standing, J.R. Field axial cyclic loading experiments on piles driven in sand. *Soils and Foundations*. 52, (2012), 723-737.

[3] R. J. Jardine, R.J. The cyclic behaviour of offshore piles. Chapter in 'The Cyclic Loading of Soils', (1991) Eds. Brown & O'Reilly, Blackie & Son, Glasgow

[4] J.T. DeJong, M.F. Randolph, D.J. White. Interface load transfer degradation during cyclic loading: a microscale investigation. *Soils and Foundations* 43 (2003), 91–94.

[5] Z.X. Yang, R.J. Jardine, B.T. Zhu, P.Y. Foray, C.H.C. Tsuha. Sand grain crushing and interface shearing during displacement pile installation in sand. *Géotechnique* 60 (2010), 469–482.

[6] R.J. Jardine, B.T. Zhu, P. Foray, & C.P. Dalton. Experimental arrangements for the investigation of soil stresses developed around a displacement pile. *Soil and Foundations* 49 (2009), 661-673.

[7] B.T. Zhu, R.J. Jardine, P. Foray. The use of miniature soil stress measuring sensors in applications involving stress reversals. *Soils and Foundations* 49 (2009), 675–688.

[8] C.H.C. Tsuha, P.Y. Foray, R.J. Jardine, Z.X. Yang, M. Silva, & S. Rimoy. Behaviour of displacement piles in sand under cyclic axial loading. *Soil and Foundations* 52 (2012), 393–410.

[9] R.J. Jardine. Some observations on the kinematic nature of soil stiffness. *Soils and Foundations* 32 (1982), 111–124.

[10] R. Kuwano, & R.J. Jardine. A triaxial investigation of kinematic yielding in sand. *Géotechnique* 57 (2007), 563–579.

[11] A. Aghakouchak, W.W. Sim., & R.J. Jardine. Stress-path laboratory tests to characterise the cyclic behaviour of piles driven in sands. Soils and Foundations companion special volume. In Press.

[12] R.J. Jardine, K. Andersen, and A. Puech. (2012). Cyclic loading of offshore piles: potential effects and practical design. Keynote Paper. Proc 7th Int. Conf. on Offshore Site Investigations and Geotechnics, SUT London, pp 59-100.